

1 Article

2 A Novel Type Room Temperature Surface Photovoltage 3 Gas Sensor Device

4 Monika Kwoka ^{1,*}, Michal A.Borysiewicz ², Pawel Tomkiewicz ³, Anna Piotrowska ², and Jacek
5 Szuber ¹

6 ¹ Institute of Electronics, Silesian University of Technology, 44-100 Gliwice, Poland; monika.kwoka@polsl.pl
7 (M.K.); jacek.szuber@polsl.pl (J.S.)

8 ² Institute of Electron Technology, 02-668 Warsaw, Poland; mbory@ite.waw.pl (M.A.B.); ania@ite.waw.pl
9 (A.P.)

10 ³ SemiInstruments Company, 41-800 Zabrze, Poland; ptomkiewicz@semiinstruments.com (P.T.)

11 * Correspondence: monika.kwoka@polsl.pl; Tel.: +48-32-237-20-57

12

13 **Abstract:** In this paper a novel type of a highly sensitive gas sensor device based on the surface
14 photovoltage effect is described. The developed surface photovoltage gas sensor is based on a
15 reverse Kelvin probe approach. As the active gas sensing electrode the porous ZnO nanostructured
16 thin films are used deposited by the direct current (DC) reactive magnetron sputtering method
17 exhibiting the nanocoral surface morphology combined with an evident surface nonstoichiometry
18 related to the unintentional surface carbon and water vapor contaminations. Among others, the
19 demonstrated SPV gas sensor device exhibits a high sensitivity of 1 ppm to NO₂ with a signal to
20 noise ratio of about 50 and a fast response time of several seconds under the room temperature
21 conditions.

22 **Keywords:** room temperature gas sensor, surface photovoltage effect, porous ZnO nanostructured
23 thin films

24

25 1. Introduction

26 Despite more than 50 years of development, the resistive type gas sensors systems based on
27 metal oxide (MOX) materials still exhibit some critical, fundamental limitations [1-4], which can be
28 divided into two groups.

29 The first one concerns the analytically useful characteristics limited to good sensitivity (usually
30 at the level of single ppm, strongly depending on the gas) with a rather poor selectivity (strongly
31 dependent on humidity, that can be improved by noble catalytic metals), as well as poor dynamic
32 parameters such as a long response time (tens of seconds) combined with a rather very long recovery
33 time (single minutes). The latter is especially relevant when compared to the responsiveness of
34 animal and human olfaction [5,6].

35 The second group concerns mainly the high temperature working conditions, usually in the
36 range of 200÷400°C causing high power consumption in the devices, combined with their limited
37 reversibility (stability), adversely affecting their costs of fabrication and possible commercialization
38 [7,8].

39 In the recent years some innovative ideas appeared in the literature how to overcome these
40 limitations including the unsolved technical and technological problems.

41 One such concerns applying various dimensionalities of the gas sensing materials. Nanoscale MOX
42 materials and fabrication technologies have allowed the fabrication of novel type sensing
43 architectures, what additionally helped to broaden the fundamental understanding of their sensing
44 mechanism [8-13]. However, despite more than one decade of studies the useful MOX characteristics
45 including sensitivity (only about 1 order better with respect to 3D thin films or even 2D nanolayers)
46 and selectivity combined with the dynamic parameters such as response/recovery times (only
47 slightly shorter with respect to 3D thin films/ 2D nanolayers) are still below the common
48 expectations [12,13].

49 A second way concerns the application of selected metal oxides for specific gases based on their
50 better specific response in terms of the above mentioned analytical characteristics. It should be
51 underlined that up to now tin dioxide, SnO₂, is the most popular gas sensor material (~ 40% of
52 papers, 60% of commercial gas sensors). However, in the last few years zinc oxide, ZnO, appeared as
53 second common gas sensor material (~20% papers). This is due to the fact that its electron mobility is
54 at the level of ~10² [cm²/V·s] similar to SnO₂, while the electron conductivity is at the level of 10³
55 [1/Ω·cm], what is one order higher than SnO₂ [12-15].

56 A third way concerns using of novel type sensing transduction principles or innovative
57 transducers using flexible sensors with smart textiles, as well as new sensing architectures including
58 Schottky-contact nanosensor, FET chemical sensors, surface ionization sensors and magnetic gas
59 sensors as recently reviewed by Comini [16].

60 However, within these ideas the influence of the work function variation and related effects on
61 gas sensing have been ignored. Perhaps it was related to the fact that these effects are based
62 essentially on the variation of contact potential difference (CPD) using mainly Kelvin vibrating
63 capacitor, what was already commonly used as the gas sensors transduction since many years
64 [17,18]. Moreover, it is also well known, that this method exhibits a rather poor sensitivity because of
65 a low signal to noise (S/N) ratio, and that this method was mainly applied for studies of porous
66 semiconductor materials [19-21]. This is probably the reason why up to now only an
67 incomprehensibly weak attention was given to the use in gas sensors of the effect of work function
68 variation of gas sensing materials (including MOX) after external optical excitation in the so called
69 surface photovoltage effect [22].

70 In general, the surface photovoltage (SPV) is defined as a change of the surface potential barrier
71 upon illumination, which is related to a photon induced charge generation and redistribution
72 within the Space Charge Region (SCR) of the semiconductor. The surface potential variations may be
73 measured with the commonly known Kelvin probe technique after external illumination. What is
74 crucial, the SPV effect mainly depends on the incident photon energy with respect to the band-gap of
75 the semiconductor under investigation and the light intensity [22].

76 Even sub-band gap photons can modify the charge at the semiconductor surfaces by exciting
77 the trapped carriers at a well defined energy, i.e. when using the photons of energy $h\nu = E_C - E_A$ or
78 $h\nu = E_A - E_V$, where E_C and E_V are the energy of bottom of conductive band and the top of valence
79 band at the surface, respectively, whereas the E_A is the energy level of traps induced by adsorbed gas
80 species, the specific electron transitions from a surface state to the conduction band (or from the
81 valence band to the surface states) can be observed. In both cases the variation of band bending at

82 the semiconductor surfaces is observed, corresponding to the variation of surface potential, what can
83 finally be measured as the variation of work function.

84 These two specific effects are the base of the so-called Surface Photovoltage Spectroscopy (SPS)
85 method [22] commonly used for many years to detect electronic states in the band gap originating
86 from semiconductor surfaces commonly used for control of quality of semiconductor surfaces in
87 aspect for their potential application in solid state microelectronics [23]. What is crucial, when
88 using the photons of energy $h\nu$ higher than band gap E_{bg} ($h\nu > E_{bg}$) this effect of variation of band
89 bending (surface potential and subsequent work function) at the semiconductor surfaces is evidently
90 stronger [22].

91 It should be pointed out that, according to the available literature, recently there were only
92 limited attempts of using the photovoltaic effects in gas detection. However, in these studies
93 performed mainly by the group of Yamada [24-26], mistakenly called as surface photovoltage effect,
94 only the photocurrent was measured across the MIS structures based on mesoporous silica films
95 exposed to limited toxic gases like NO and NO₂. Moreover, what is also puzzling, there has been
96 only limited interest of using the true SPV effect even in the basic studies of gas interaction with
97 MOX materials [27,28], without any reference to use this effect potentially for the toxic gas detection.
98 This is why in our group, having significant experience in the use of very high sensitivity SPV effect
99 for the control of quality of semiconductor surfaces in contact with different atmospheres [23], the
100 systematic studies focusing on the application of SPV for the control of interaction of toxic gases
101 with selected MOX gas sensor materials have been lately carrying out. As the result of these studies,
102 a novel type of a room temperature gas sensor device utilizing a sensing mechanism based on the
103 measurements of the SPV effect on porous nanostructures ZnO electrodes was developed.

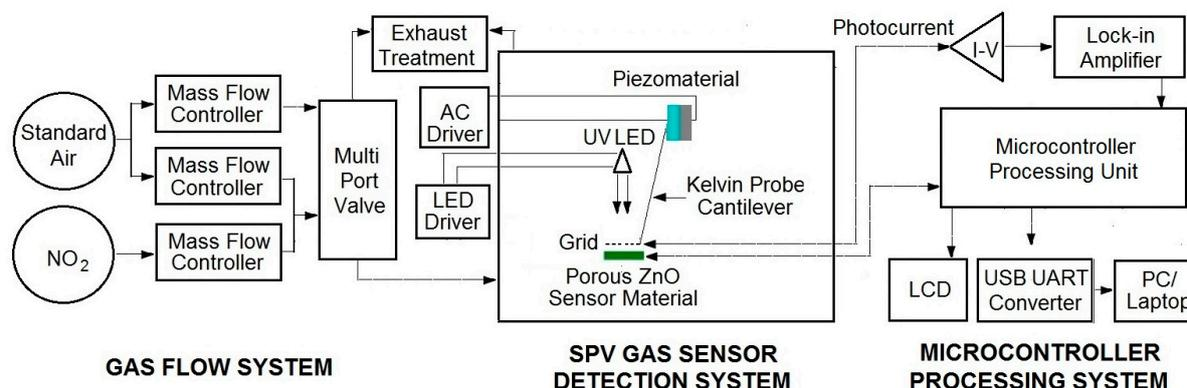
104 In this paper the details of above mentioned SPV gas sensor system based on porous ZnO
105 nanostructured thin films are described. However, at the beginning, the fundamental
106 physicochemical properties of porous ZnO nanostructured thin films were analyzed with a special
107 emphasis on the local surface chemistry and morphology, absolutely indispensable for the
108 interpretation of basic analytical sensing parameters of the elaborated novel type SPV gas sensor
109 system.

110 2. Materials and Methods

111 As was mentioned above, in the constructed gas sensor device porous ZnO nanostructured thin
112 films were used as the sensor material. They were deposited onto Si (100) substrates by direct
113 current (DC) reactive magnetron sputtering of a 99.95%-pure Zn target in an 6N argon-oxygen
114 sputtering mixture at oxygen concentration of 33% under total working pressures of 1.5 mTorr,
115 using the Surrey NanoSystems 1000C reactor. After deposition, the ZnO films were annealed *ex situ*
116 in a 6N-pure oxygen flow at 800 °C using a Mattson SHS-100 rapid thermal processing (RTP)
117 furnace. Other technological details combined with the results of fundamental characterization of
118 their bulk chemistry and morphology by chosen experimental methods performed at the Institute of
119 Electron Technology, Warsaw, Poland, have been already described elsewhere [29,30].

120 Having in mind our recent experiences in studies of tin dioxide SnO₂ thin films nanostructures
121 as the commonly used oxide gas sensor material [31], the local surface chemistry of these porous
122 ZnO nanostructured thin films was controlled by X-ray Photoelectron Spectroscopy (XPS) method at
123 the Institute of Electronics, Silesian University of Technology, Gliwice, Poland. The experimental
124 details of XPS studies have recently been described in our recent paper [32].

125 The elaborated surface photovoltage (SPV) gas sensor system contains of 3 main parts, as
 126 shown in **Figure 1**.



127

128 Figure 1. Simplified block-scheme of elaborated surface photovoltage (SPV) gas sensor system (device).

129 Apart from the typical gas flow system containing selected gases, mass flow controllers with
 130 multiport valve, it contains the SPV gas sensor detection system combined with microcontroller
 131 processing system for data processing and acquisition.

132 The elaborated SPV gas detection system is based on the reverse Kelvin probe flat type
 133 vibrating capacitor system. The capacitor subsystem consists of the porous ZnO nanostructured thin
 134 films as a flat gas sensor material playing the role of the active electrode, combined with the
 135 reference flat Cu metallic grid-type electrode on specific vibrating cantilever after piezoelectric
 136 driving using AC voltage generator.

137 The alternating SPV signal is measured as the variation of work function of the gas sensor
 138 material (with respect to the vibrating reference Cu electrode) as the result of its surface band
 139 bending variation after UV illumination by a UV5-400-30 type LED diode (Bivar Company). It
 140 should be pointed out that the alternating SPV signal can also be measured using the static reference
 141 Cu electrode combined with UV LED light modulated by respective driver. However, the latest
 142 approach does not allow the phenomena recognition that is responsible for the surface potential
 143 change. In other words, at the complex gas sensor system, the potential barrier is a sum of a fixed
 144 charge potential that may arise from the adsorbed species, strict surface region gas molecule
 145 reorganization, and carrier generation and redistribution in the SCR region.

146 For the measuring and acquisition of the SPV signal response in selected gases the
 147 microcontroller processing system is used containing the data processing control unit working with,
 148 among others, the I/V photocurrent converter (amplifier), the respective DAC and ADC converters,
 149 and finally the zero self-compensating lock-in amplifier for the reverse Kelvin probe flat vibrating
 150 capacitor system. Moreover, microcontroller processing system is equipped with USB to UART
 151 converter for laptop connection, enabling the use of our SPV gas sensor system as a mobile device.

152 In our test experiments of the elaborated SPV gas sensor system (device) a mixture of pure
 153 nitrogen dioxide NO₂ in standard synthetic air was used at different concentrations.

154 3. Results and Discussion

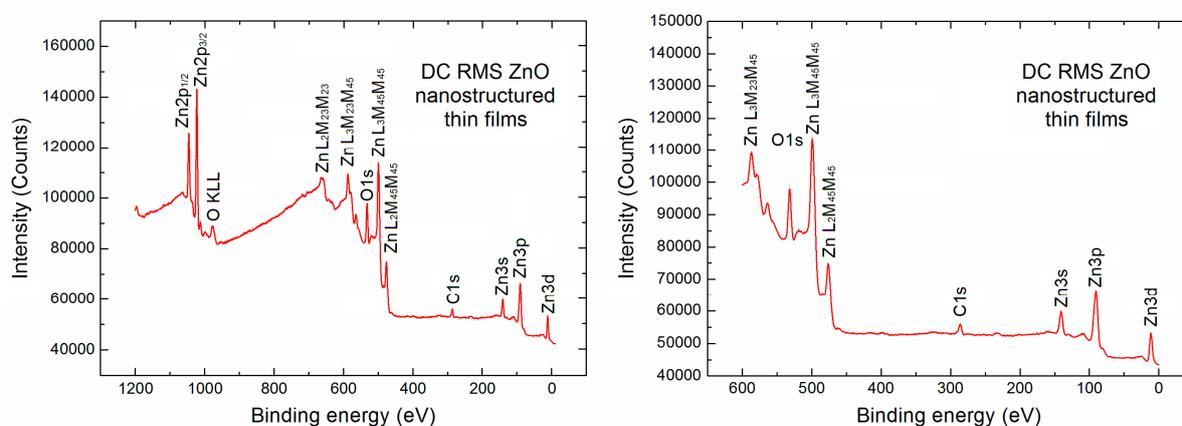
155 As was mentioned above in our SPV gas sensor system the porous ZnO nanostructured thin
 156 films deposited onto Si (100) substrate was used as the gas sensing material for which the bulk

157 chemistry and morphology have been characterized by chosen experimental techniques [29], as
 158 shortly summarized below.

159 Using the Rutherford Backscattering Spectroscopy (RBS) it was shown that the obtained ZnO
 160 layers were almost stoichiometric with the oxygen to zinc atomic ratio close to 1. In turn, using the
 161 Scanning Electron Microscopy (SEM) it was observed from the cross-sectional images, that the
 162 obtained ZnO layers exhibit nanocoral morphologies as shown in [29] Their polycrystalline
 163 character was also confirmed by X-ray Diffraction (XRD) showing powder diffraction patterns, also
 164 described in [29]. However, since from our experience with SnO₂ nanostructures we know that they
 165 contain a significant surface nonstoichiometry related to undesired strong surface carbon and water
 166 vapor contaminations, the additional XPS studies of the local surface chemistry our porous ZnO
 167 nanostructured thin films have additionally been performed. Such information is absolutely
 168 indispensable when trying to understand the gas sensing mechanism since the sensor effect appears
 169 just on the surface of the gas sensing materials at the depth related to Debye length [12,13], which is
 170 quite similar to the information depth of XPS method. The obtained XPS results are shortly
 171 described and interpreted below.

172 3.1. Local surface chemistry of the porous ZnO nanostructured thin films

173 At the beginning the XPS survey spectrum for the porous ZnO nanostructured thin films used
 174 in our SPV gas sensor device has been recorded shown in **Figure 2** in two various binding energy
 175 ranges.



176

177 Figure 2. XPS survey spectra (full and in limited 600 eV BE range) of the ZnO nanostructured thin films used in
 178 our SPV gas sensor.

179 On the left side a typical full XPS survey spectrum in the binding energy (BE) range
 180 (1200 eV) is visible, what confirms that apart from the Auger electron lines (can be usually skipped)
 181 the contribution from the basic elements of ZnO derived from the respected XPS core level Zn2p,
 182 O1s, Zn3s, Zn3p and Zn3d lines is observed. Moreover, what is crucial in our studies, an evident
 183 undesired contribution of the C1s XPS lines at BE ~ 286.0 eV is observed, what confirms that the
 184 strong undesired C contamination exists at the surface of porous ZnO nanostructured thin films
 185 used in our SPV gas sensor device.

186 Commonly, basing on the relative intensity (height) of Zn2p, O1s and C1s core level lines and
 187 the well known analytical formula [33-35] and the respective atomic sensitivity factors related to the
 188 height of the above mentioned Zn2p, O1s and C1s peaks, the relative concentration of the selected
 189 elements can be calculated. However, because of the undesired high background in our observed
 190 XPS full survey spectrum of 1200 eV binding energy (BE) range with the additional useless Auger
 191 electron emission lines, the relative concentration of main elements at the surface of porous ZnO
 192 nanostructured thin films has also been estimated on the base of survey spectra in the limited
 193 binding energy range (600 eV) (right side in Fig.2).

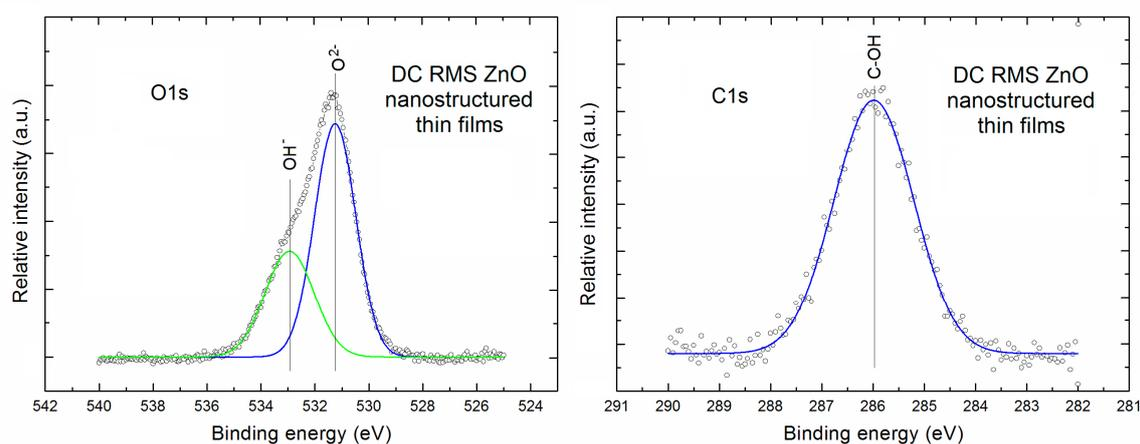
194 Our calculation showed that our porous ZnO nanostructured thin films were rather far from the
 195 surface stoichiometry. The relative [O]/[Zn] and [C]/[Zn] concentration reached the values 0.63 and
 196 0.31, respectively. It means that this is in an evident contrary to the information obtained by using
 197 the RBS method, where the oxygen to zinc atomic ratio was close to 1. This is probably related to the
 198 different information depth of both methods because for the RBS method it is at the level of
 199 hundreds of nm, whereas for XPS it corresponds only to the subsurface region of depth at the level
 200 of ~ 3 nm [33-35].

201 The different information depth was probably a reason that an evident C contamination was
 202 observed by XPS in our studies for our porous ZnO nanostructured thin films (with relative C)/[Zn]
 203 concentration of ~ 0.31), what was impossible by using the RBS method.

204 This is why at the next step of our analysis we have focused on the local surface chemistry of
 205 our porous ZnO nanostructured thin films, with a special emphasis on the specific surface bondings.

206 Our analysis was based on the deconvolution procedure of O1s and C1s spectral lines using the
 207 Casa XPS SPECS software. The obtained results are described below.

208 **Figure 3** presents the XPS O1s and C1s lines after deconvolution using Gauss fitting ((left and
 209 right column, respectively) for the porous ZnO nanostructured thin films.



210
 211 Figure 3. The XPS O1s and C1s lines after deconvolution using Gauss fitting procedure for the porous ZnO
 212 nanostructured thin films.

213 It is clearly visible, that the XPS O1s line of our porous ZnO nanostructured thin films is
 214 evidently asymmetric. After Gauss deconvolution (with very high line fitting (RMS ~ 0.998))
 215 it consists of two evident components. A first one is located at the binding energy of ~ 531.2 eV and
 216 can be attributed to the O²⁻ ions in ZnO lattice of our porous ZnO nanostructured thin films, whereas
 217 a second one at binding energy ~ 532.9 eV can be attributed to the oxygen atoms in OH- groups at the

218 surface of our porous ZnO nanostructured thin films. The similar two above mentioned components
219 of the O1s XPS line was recently observed, among other, by Gazia et [36] for the spongelike
220 nanostructured ZnO films deposited from the sputtered nanostructured zinc films. In addition, on
221 the base of deconvoluted XPS O1s line the relative area of specific components in to O²⁻ ions with
222 respect to the surface OH groups was determined as equal to 1.85, what means that even at the
223 surface there is domination of O²⁻ ions related to ZnO crystalline lattice.

224 In turn, the XPS C1s line of our porous ZnO nanostructured thin films is practically symmetric.
225 After its Gauss deconvolution (with high line fitting (RMS ~ 0.98)) it contains only one component
226 always being observed at the binding energy of ~ 286 eV, what can be attributed to the C-OH surface
227 bondings, commonly observed at the surface of various metal oxides, what is easy available in the
228 NIST X-ray Photoelectron Spectroscopy Database [37].

229 Taking all above into account, what is crucial, it should be underlined, that in our experiments
230 the existence of undesired water vapor combined with carbon contaminations at the surface of our
231 porous ZnO nanostructured thin films having the nanocrystalline, columnar structures of cross
232 section in the range of several nm [29], cannot be ignored when their sensing properties are
233 analyzed. This is crucial because this information, probably well undesired and commonly ignored
234 in the available literature, will be additionally commented in the next chapter, where the gas sensor
235 characteristics of our novel type gas sensor system (device) will be analyzed.

236 *3.2. Gas sensing characteristics in NO₂ atmosphere*

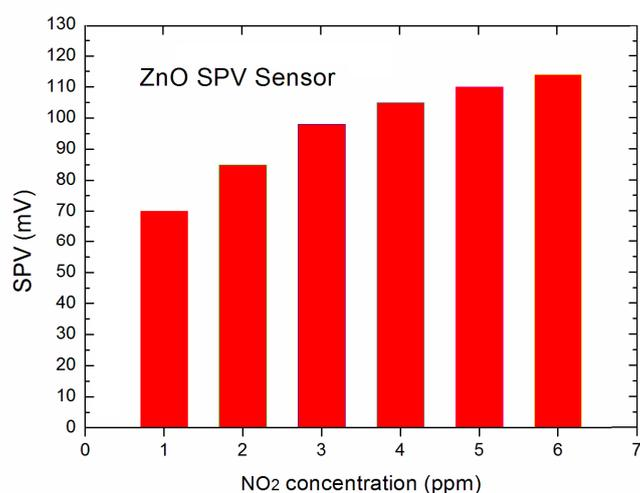
237 As was mentioned above the porous ZnO nanostructured thin films were used as the static
238 electrode in the gas sensor system (device) using the surface photovoltage effect. As was mentioned
239 above, the gas detection effect is based on the variation of ZnO surface charge and subsequent
240 surface potential due to the interaction of toxic NO₂ gas with our gas sensor material.

241 Already the primary experiments proved our expectations that our novel type SPV gas sensor
242 system is working at room temperature. However, to reach the constant primary surface potential
243 and subsequent constant starting value of SPV signal allowing the repeatable working conditions
244 of our system the standard dry synthetic air was flowing via the system for several hours. It was
245 related to the fact that only in such conditions there is a real chance for the removing of undesired
246 water vapor molecules physically adsorbed at the surface of our gas sensor materials being
247 previously in the natural air (usually wet) atmosphere.

248 Only after that we have focused on the registration of variation of SPV signal with variation of
249 the concentration of active gas NO₂ in the standard dry synthetic air. In this experiments we have
250 focused on two aspects.

251 On the base of registration of the relative variation of SPV signal as a function of NO₂
252 concentration the detection threshold of our SPV gas sensor system (related to its sensitivity) was
253 determined, combined with the analysis of their dynamic characteristics like response time and
254 respected recovery time at specific NO₂ concentrations.

255 Our experiments showed that the elaborated novel type SPV gas sensor system allows the detection
256 of NO₂ gas up to 1 ppm, at the signal to noise (S/N) ratio at the level ~ 50. The obtained data for the
257 lowest, selected NO₂ gas concentration in the main range of 1÷5 ppm were taken down in the form of
258 diagram shown in **Figure 4**.



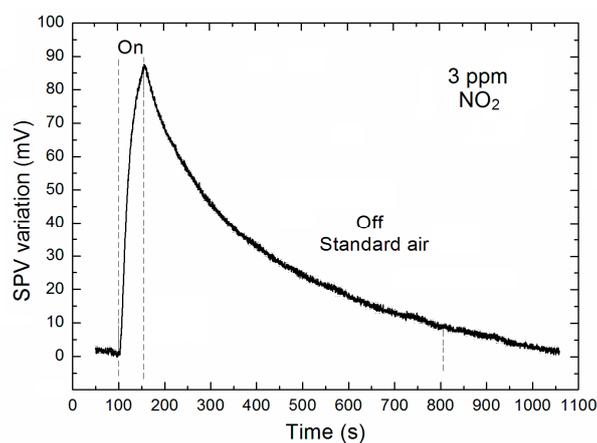
259

260 Figure 4. The variation of SPV signal as a function of NO₂ concentration.

261 At this point it should be underlined that perhaps our system is able to detect the NO₂ gas
 262 detection below 1 ppm, since the signal to noise (S/N) ratio was at the level ~ 50, but our gas flow
 263 system (shown in Fig.1) was only able to work in repeatable and reliable measuring condition only
 264 up to 1 ppm. Nevertheless, the obtained results look very promising having in mind that our strong
 265 SPV signal even at 1 ppm of NO₂ was reached already at room temperature working conditions. This
 266 is not possible by using the common resistive type gas sensor based on various forms of ZnO as gas
 267 sensor material [12,13]. Moreover, it should be also underlined that the respective, relative
 268 sensitivity is even at room temperature of about 1 order better with respect to commonly used
 269 various forms of ZnO thin films working at evidently higher temperature in the range of 200-350° C
 270 [12,13]. This is extremely important advantage of our SPV gas sensor system having in mind that the
 271 high concentration of undesired H₂O vapor and C surface contaminations at the surface of our gas
 272 sensing material can play a role of evident barrier for the more effective gas sensing effect.

273 As was mentioned above, at the next step of our experiments we have focused on the
 274 determination of dynamic characteristics of our SPV gas sensor system including response time and
 275 respected recovery time at specific NO₂ concentrations. The obtained results look promising.

276 **Figure 5** shows the time dependent variation of SPV signal related to the dynamic parameters
 277 for the middle value of NO₂ concentration (3 ppm) within the recently mentioned its main range
 278 used in our experiments.



279

280 Fig.5. The variation of SPV signal as a function of time for the 3 ppm NO₂ concentration.

281 As it is commonly accepted in literature, the respective gas sensor dynamic characteristics
 282 (response and recovery times, respectively) are defined as the respective time at which the signal
 283 reaches 90% value of its full relative variation. Taking it into account it is clearly visible that for 3
 284 ppm NO₂ concentration the response time is at the level of about 50 s. Its estimated values for all
 285 other NO₂ concentration used in our experiments are summarized in Table I. What is important, as
 286 mentioned above, the response time varies in the range of 52 ÷ 24 s for the variation of NO₂
 287 concentration the our main range of 1÷5 ppm, respectively.

288 Of course, these values are not spectacular with respect to the commonly used the resistive type
 289 gas sensor based on various forms of ZnO as gas sensor material. However, it looks very promising
 290 since was obtained already at the room temperature working conditions.

291 What concern the second dynamic parameter - recovery time, it look not so promising because
 292 for the 3 ppm NO₂ concentration it is at the level of about 680 s (~11 mins). Its estimated values for
 293 all other NO₂ concentration used in our experiments are also summarized in **Table I**.

294 **Table I.**

295 Response time and respective recovery time of SPV signal of our SPV gas sensor device for the main range of
 296 NO₂ concentration used in our experiments.

SPV gas sensor dynamic parameters	NO ₂ concentration [ppm]				
	1	2	3	4	5
Response time [s]	52	42	38	30	24
Recovery time [s]	~1500	900	680	580	500

297 However, what should be also underlined the recovery time triply decreases for the variation of
 298 NO₂ concentration the range of 1÷5 ppm, respectively. Of course, it looks rather poor as considerably
 299 long. However, it has already been reached when leaving the porous ZnO nanostructured thin films
 300 in the standard synthetic air at room temperature, without any additional regeneration effects. This
 301 observation can be treated as the direct proof that the target gas was only physically adsorbed onto
 302 the inner surfaces of the porous ZnO nanostructured thin films having the columnar type
 303 morphology. As a consequence, because the adsorption/desorption process of the NO₂ gas at the
 304 surface of our gas sensor material is rather slow, it causes that the better dynamic characteristics
 305 cannot be expected. However, it should be pointed out that probably even very slow regeneration
 306 effect of gas sensor material in the dry standard synthetic air was additionally enhanced by the
 307 continuous irradiation of our porous ZnO nanostructured thin films by the UV-LED source used in
 308 our SPV experiment, what can lead to the small drift of gas sensor material temperature. This is why
 309 our SPV gas sensor system exhibits natural tendency to even slow auto-regeneration.

310 The regeneration effect can be additionally improved by using the additional IR-LED source.
 311 Our primary experiments are very promising in this aspect since the recovery time can be reduced
 312 by factor 5. Nevertheless, it needs additional experiments for the determination of precise conditions
 313 of the precisely controlled thermal regeneration (self-heating) of our porous ZnO nanostructured
 314 thin films after exposure to the target gases. Perhaps this self-heating effect can improve the
 315 sensitivity of our SPV gas sensor system, what was additionally observed at higher NO₂
 316 concentration. However, this last approach slightly decreases the main advantage of our SPV gas

317 sensor system, i.e. room temperature working conditions during both the exposure of gas sensor
318 material to target gas and its subsequent regeneration, without any additional external device like
319 power supply. Nevertheless, it can be consider as an option in aspect for their potential future
320 commercialization. Nowadays, the electronic progress allow for further miniaturization by applying
321 the ready on chips IC's that increase importance of studying novel examination techniques like a
322 reverse Kelvin probe approach.

323 5. Conclusions

324 In our studies a novel type room temperature surface photovoltage (SPV) gas sensor system
325 based on the reverse Kelvin probe with vibrating grid type electrode and porous ZnO
326 nanostructured thin films system has been successfully developed.

327 The initial XPS experiments showed that for our porous nanostructured ZnO thin films an
328 evident surface nonstoichiometry is observed combined with the high undesired H₂O vapor and
329 C surface contaminations.

330 In turn, our gas sensing experiments showed, among others, that the elaborated surface
331 photovoltage gas sensor system exhibits a relatively high sensitivity in NO₂ atmosphere (up to 1
332 ppm at signal to noise ratio ~50) and relatively fast response time (~ several seconds). Having
333 identified undesired H₂O vapor and C surface contaminations, we can see a potential for
334 performance improvement, when the contaminants are removed. The presented device is
335 significantly advantageous over the commonly used resistance type MOX gas sensor not only by
336 using the nondestructive SPV effect measurements, but most importantly by operation at room
337 temperature.

338 In currently ongoing works we aim at improving the sensor system performance, in particular
339 by increasing the sensitivity and shortening the response and recovery times. We plan to test
340 heat-cleaning of the electrode by additional IR-LED source and to study other ZnO/MOX
341 nanostructures with extended internal surfaces for the more effective adsorption/desorption effects
342 of target gasses during the gas sensor working conditions.

343 **Author Contributions:** Conceptualization, M.K. and J.S.; Methodology, P.T.; Software, P.T.; Investigation, M.K.
344 and M.A.B.; Writing-Original Draft Preparation, M.K., M.A.B.; Writing-Review & Editing, J.S.; Supervision,
345 M.K., J.S.; Project Administration, M.K, J.S., A.P.; Funding Acquisition, M.K and A.P.

346 **Funding:** Works on SPV gas sensor device have been supported by the Project InTechFun realized within the
347 Operational Programme of Innovative Economy - POIG.01.03.01-00-159/08, founded by European Union within
348 the European Regional Development Fund. However, the main part of results presented in this paper have been
349 obtained within the realization of research grant of National Science Centre, Poland - OPUS 11, no
350 2016/21/B/ST7/02244

351 **Conflicts of Interest:** The authors declare no conflict of interest.

352 References

- 353 1. Göpel, W.; Reinhardt, W. Metal Oxide Sensors: New Devices Through Tailoring Interfaces on the Atomic
354 Scale, in *Sensors Update*, WILEY-VCH Verlag GmbH, Weinheim, **1996**, Vol.1, Issue1, 49-120.
355 [doi.org/10.1002/1616-8984\(199607\)1:1](https://doi.org/10.1002/1616-8984(199607)1:1).
- 356 2. Barsan, N.; Koziej, D.; Weimar, U. Metal oxide-based gas sensor research: How to? *Sensors and Actuators B*
357 **2007**, *121*, 18–35. doi.org/10.1016/j.snb.2006.09.047.
- 358 3. Comini, E.; Faglia, G.; Sberveglieri G. Electrical-based Gas Sensing, in *Solid State Gas Sensing*, Comini, E.;
359 Faglia, G.; Sberveglieri G., Eds., Springer, New York, **2009**, 47-108, ISBN: 978-0-387-09664-3.

- 360 4. Fine, G.F.; Cavanagh, L.M.; Afonja, A.; Binions, R. Metal Oxide Semi-Conductor Gas Sensors in
361 Environmental Monitoring, *Sensors* **2010**, *10*, 5469-5502. doi:10.3390/s100605469.
- 362 5. Gardner, J.; Bartlett, Ph.N. *Sensors and Sensory Systems for an Electronic Nose*, Springer Sci. Media, 2013.
- 363 6. *The Electronic Nose: Artificial Olfaction Technology*, Ed. Patel, H.K. Springer Sci. & Business Media, India, 2016.
- 364 7. Simon, I.; Barsan, N.; Bauer, M.; Weimar, U. Micromachined metal oxide gas sensors: opportunities to
365 improve sensor performance, *Sensors and Actuators B* **2001**, *73*, 1-26. doi.org/10.1016/S0925-4005(00)00639-0.
- 366 8. Korotcenkov, Gh. New Trends and Technologies, in *Handbook of Gas Sensor Materials: Properties, Advantages*
367 *and Shortcomings for Applications*. Vol.2, Springer, 2014, 47-71.
- 368 9. Comini, E.; Baratto, C.; Faglia, G.; Ferroni, M.; Vomiero, A.; Sberveglieri, G. Quasi one dimensional metal
369 oxide semiconductors: preparation, characterization and application as chemical sensors, *Progr. Mater. Sci.*
370 **2009**, *54*, 1-67. doi.org/10.1016/j.pmatsci.2008.06.003.
- 371 10. Vander Wal, R.L.; Berger, G.M.; Kulis, M.J.; Hunter, G.W.; Xu, J.C.; Evans, L. Synthesis Methods, Microscopy
372 Characterization and Device Integration of Nanoscale Metal Oxide Semiconductors for Gas Sensing, *Sensors*
373 **2009**, *9*, 7866-7902. doi:10.3390/s91007866.
- 374 11. Baratto, C.; Comini, E.; Faglia, G.; Sberveglieri, G. The Power of Nanomaterial Approaches in Gas Sensors, in
375 *Solid State Gas Sensors: Industrial Application*, M. Fleischer and M. Lehmann (Eds.), Springer Series on
376 Chemical Sensors and Biosensors, Springer-Verlag, Berlin-Heidelberg, 2011, 53-78. DOI 0.1007/5346 2011 3
- 377 12. Eranna, G. *Metal oxide nanostructures as gas sensing devices*, CRC Press, Boca Raton, 2012.
- 378 13. Carpenter, M.A.; Mathur, S.; Kolmakov, A. *Metal oxide nanomaterials for chemical sensors*, Springer, New York,
379 2012. ISBN: 146145395X, 9781461453956.
- 380 14. *Zinc Oxide: Bulk, Thin Films and Nanostructures*, Ch.Jagadish, S.J.Pearton (Eds.) Elsevier, Amsterdam, 2006.
- 381 15. *Oxide and Nitride Semiconductors: Processing, Properties and Applications*, Eds. Yao, T.; Hong, S.-K., Springer,
382 Berlin, 2009. ISBN: 978-3-540-88846-8.
- 383 16. Comini, E. Metal oxide nanowire chemical sensors: innovation and quality of life, *Materials Today* **2016**, *19*
384 559-567. doi.org/10.1016/j.mattod.2016.05.016
- 385 17. Mizsei, J.; Harsanyi, J. Resistivity and work function measurements on Pd-doped SnO₂ sensor surface,
386 *Sensors and Actuators* **1983**, *4*, 397-402. doi.org/10.1016/0250-6874(83)85050-1.
- 387 18. Mizsei, J.; Lantto, V. Simultaneous response of work function and resistivity of some SnO₂-based samples
388 to H₂ and H₂S, *Sensors and Actuators B* **1991**, *4*, 163-168. doi.org/10.1016/0925-4005(91)80193-N.
- 389 19. Mizsei, J. Vibrating capacitor method in the development of semiconductor gas sensors, *Thin Solid Films*,
390 **2005**, *490*, 17-21. doi.org/10.1016/j.tsf.2005.04.021.
- 391 20. Oprea, A.; Barsan, N.; Weimar, U. Work function changes in gas sensitive materials: Fundamentals and
392 applications, *Sensors and Actuators B* **2009**, *142*, 470-493. doi.org/10.1016/j.snb.2009.06.043.
- 393 21. Korotcenkov, Gh.; Cho, B.K. Porous Semiconductors: Advanced Material for Gas Sensor Applications, *Crit.*
394 *Rev. Solid State Mater. Sci.* **2010**, *35*, 1-37. doi.org/10.1080/10408430903245369.
- 395 22. Kronik, L.; Shapira, Y. Surface photovoltage phenomena: theory, experiments, and applications, *Surface*
396 *Science Report* **1999**, *37*, 1-206. doi.org/10.1016/S0167-5729(99)00002-3.
- 397 23. Tomkiewicz, P.; Arabasz, S.; Adamowicz, B.; Miczek, M.; Mizsei, J.; Zahn, D.R.T.; Hasegawa, H.; Szuber, J.
398 Surface electronic properties of sulfur-treated GaAs determined by surface photovoltage measurement and
399 its computer simulation, *Surface Science* **2009**, *603*, 498-502. doi.org/10.1016/j.susc.2008.12.009.
- 400 24. Zhou, H.-S.; Yamada, T.; Asai, K.; Honma, I.; Uchida, H.; Katsube, T. NO Gas Sensor Based on Surface
401 Photovoltage System Fabricated by Self-Ordered Hexagonal Mesoporous Silicate Film, *Jpn. J. Appl. Phys.*
402 **2001**, *40*, 7098-7102. DOI: 10.1143/JJAP.40.7098

- 403 25. Yamada, T.; Zhou, H.S.; Uchida, H.; Tomita, M.; Ueno, Y.; Honma, I.; Asai, K.; Katsube, T. Application of a
404 cubic-like mesoporous silica film to a surface photovoltage gas sensing system, *Microporous and Mesoporous*
405 *Materials* **2002**, *54*, 269–276. [doi.org/10.1016/S1387-1811\(02\)00387-6](https://doi.org/10.1016/S1387-1811(02)00387-6).
- 406 26. Yulianto, B.; Zhou, H.S.; Yamada, T.; Honma, I.; Katsumura, Y.; Ichihara, M. Effect of Tin Addition on
407 Mesoporous Silica Thin Film and Its Application for Surface Photovoltage NO₂ Gas Sensor, *Anal. Chem.*
408 **2004**, *76*, 6719–6726. [DOI: 10.1021/ac0495642](https://doi.org/10.1021/ac0495642).
- 409 27. Rothschild, A.; Levakov, A.; Shapira, Y.; Ashkenasy, N.; Komem, Y. Surface photovoltage spectroscopy
410 study of reduced and oxidized nanocrystalline TiO₂ films, *Surface Science* **2003**, 532–535, 456–460.
411 [doi:10.1016/S0039-6028\(03\)00154-7](https://doi.org/10.1016/S0039-6028(03)00154-7).
- 412 28. Sivalingam, Y.; Magna, G.; Pomarico, G.; Martinelli, E.; Paolesse, R.; D'Amico, A.; Di Natale, C. Gas effect on
413 the surface photovoltage of porphyrins functionalized ZnO nanorods, *Adv.Mater.Lett.* **2012**, *3*, 442–448.
414 [DOI: 10.5185/amlett.2012.icnano.144](https://doi.org/10.5185/amlett.2012.icnano.144).
- 415 29. Borysiewicz, M.A.; Dynowska, E.; Kolkovsky, V.; Dyczewski, J.; Wielgus, M.; Kaminska, E.; Piotrowska, A.
416 From porous to dense thin ZnO films through reactive DC sputter deposition onto Si (100) substrates,
417 *Phys. Status Solidi A* **2012**, *209*, 2463–2469. doi.org/10.1002/pssa.201228041.
- 418 30. Maslyk, M.; Borysiewicz, M.A.; Wzorek, M.; Wojciechowski, T.; Kwoka, M.; Kaminska, E. Influence of
419 absolute argon and oxygen flow values at a constant ratio on the growth of Zn/ZnO nanostructures obtained
420 by DC reactive magnetron sputtering, *Applied Surface Science* **2016**, *389*, 287–293.
421 doi.org/10.1016/j.apsusc.2016.07.098
- 422 31. Kwoka, M.; Ottaviano, L.; Szuber, J. Comparative analysis of physicochemical and gas sensing
423 characteristics of two different forms of SnO₂ films, *Applied Surface Science* **2017**, *401*, 256–261;
424 doi.org/10.1016/j.apsusc.2016.12.205.
- 425 32. Kwoka, M.; Lyson-Sypien, B.; Kulis, A.; Maslyk, M.; Borysiewicz, M.A.; Kaminska, E.; Szuber, J. Surface
426 Properties of Nanostructured, Porous ZnO Thin Films Prepared by Direct Current Reactive Magnetron
427 Sputtering, *Materials* **2018**, *11*, 131. [doi:10.3390/ma11010131](https://doi.org/10.3390/ma11010131).
- 428 33. Wagner, C.D.; Riggs, W.M.; Davis, L.E.; Moulder J.F.; Mnilenberger, G.E. *Handbook of X-ray Photoelectron*
429 *Spectroscopy*, Perkin-Elmer, Eden Prairie, MN **1979**. doi.org/10.1002/sia.740030412
- 430 34. Moulder, J.F.; Stickle, W.F.; Sobol, P.E.; Bomben, K.D. *Handbook of X-ray photoelectron spectroscopy: a reference*
431 *book of standard spectra for identification and interpretation of XPS data*, Perkin-Elmer Corp, UK, **1995**.
- 432 35. Watts, J.F.; Wolstenholme, J. *An Introduction to Surface Analysis by XPS and AES*, J.Wiley & Sons, Chichester,
433 **2003**. ISBN: 978-0-470-84713-8.
- 434 36. Gazia, R.; Chiodoni, A.; Bianco, S.; Lamberti, A.; Quaglio, M.; Sacco, A.; Tresso, E.; Mandracci, P.; Pirri, C.F.
435 An easy method for the room-temperature growth of spongelike nanostructured Zn films as initial step for
436 the fabrication of nanostructured ZnO, *Thin Solid Films* **2012**, *524*, 107–112
437 doi.org/10.1016/j.tsf.2012.09.076.
- 438 37. NIST X-ray Photoelectron Spectroscopy Database - <https://srdata.nist.gov/xps/>